Selective Dibenzothiophene Adsorption on Graphene Prepared Using Different Methods

ARTICLE *in* INDUSTRIAL & ENGINEERING CHEMISTRY RESEARCH · JULY 2012

Impact Factor: 2.59 · DOI: 10.1021/ie301209c

7 AUTHORS, INCLUDING:

Chang Hyun Ko
Chonnam National University
84 PUBLICATIONS **2,359** CITATIONS
SEE PROFILE

Wook Ahn
University of Waterloo
19 PUBLICATIONS **143** CITATIONS
SEE PROFILE

Eric Croiset
University of Waterloo
134 PUBLICATIONS **2,869** CITATIONS
SEE PROFILE

Zhongwei Chen
University of Waterloo
179 PUBLICATIONS **5,241** CITATIONS
SEE PROFILE

I&EC research
Industrial & Engineering Chemistry Research

Article

pubs.acs.org/IECR

Selective Dibenzothiophene Adsorption on Graphene Prepared Using Different Methods

Hoon Sub Song,[†] Chang Hyun Ko,*[,‡] Wook Ahn,[§,∥] Bae Jung Kim,[†] Eric Croiset,*[,†] Zhongwei Chen,[†] and Sung Chan Nam[∥]

[†]Department of Chemical Engineering, University of Waterloo, 200 University Avenue West, Waterloo, Ontario, Canada N2L 3G5
[‡]School of Applied Chemical Engineering, Chonnam National University, 77 Yongbong-ro, Buk-gu, Gwangju, Korea 500-757
[§]Department of Materials Science & Engineering, Yonsei University, 50 Yonsei-ro, Seodaemun-Gu, Seoul, Korea 120-749
[∥]Korea Institute of Energy Research, 71-2, Jang-dong, Yuseong-gu, Daejeon, Korea 305-343

ABSTRACT: Graphite oxide synthesized with phosphoric acid, labeled "GOP", shows a higher degree of oxidation and has a larger interlayer spacing than the oxide prepared using the conventional Hummers method, referred to as "GOH", as confirmed by X-ray photoelectron spectroscopy and X-ray diffraction analyses. This study was performed under the assumption that the oxygen-containing functional groups between the GOP layers are more easily reduced than those between the GOH layers. Raman analysis supported this assumption in that the reduced graphene from GOP has a larger number of sp^2 carbons and fewer defects than the graphene obtained from GOH. The relative extent of defects in graphene can be investigated by dibenzothiophene (DBT) adsorption, which requires $\pi-\pi$ interactions between the free π-bonds of sp^2 atoms from graphene and those from the aromatic ring of DBT. The graphene obtained from GOP showed higher DBT adsorption capacity than that synthesized from GOH. In addition, the DBT adsorption capacity on graphene decreased as the concentrations of other aromatic compounds increased.

1. INTRODUCTION

Graphene has received considerable attention recently because it has a single two-dimensional (2D) atomic layer (sp^2 carbon configuration) arranged in a honeycomb lattice. Many studies have been conducted to investigate the thermal[1,2] and mechanical[1,3] properties of graphene. Many studies have already focused on the properties of the graphite oxide and graphene for commercial applications, especially for rechargeable batteries or supercapacitors.[1,6,7] Graphene can be manufactured by the exfoliation of graphite powder or by epitaxial growth on silicon carbide. Graphite exfoliation can be achieved by strong oxidation of the graphite layers to yield graphite oxide (GO). GO is hydrophilic and has a continuous aromatic structure containing epoxides, alcohols, ketones, carbonyls, and carboxylic groups.[4,5] Those functional groups enable the exfoliation of the graphite layers to create the interlayer spacing, or *d*-spacing. The Hummers method[8] is generally considered to be a typical method to produce graphite oxide, and many studies have used this method or a modified version of it.[9−11] Recently, a new synthesis method has been proposed using phosphoric acid as a second acid in order to enlarge the graphene *d*-spacing layer.[12]

The degree of oxidation of graphite oxide can be controlled through the synthesis procedure. In this study, therefore, the characteristics of graphite oxides as a function of different synthesis procedures have been investigated. From an application point of view, adsorption by $\pi-\pi$ interaction is an attractive method for removing bulky thiophene compounds from diesel at ambient temperature.[13] Deep desulfurization of fuels has received considerable attention because government regulations on sulfur emissions are becoming more and more stringent. Many studies have already been performed on deep desulfurization by hydrodesulfurization (HDS) using Co/Mo or Ni/Mo for lowering the sulfur content of petroleum feedstocks.[14−17] Although the HDS process is effective in removing thiols and sulfides, it is not adequate for removing bulky sulfur compounds such as thiophene (TH), benzothiophene (BT), and dibenzothiophene (DBT). Therefore, various new adsorbents, such as zeolites, silica-based sorbents, or activated carbon, have been investigated for use in the efficient removal of sulfur from fuels. Among various desulfurization adsorbents, π-complexation adsorbents (stronger than van der Waals interactions) are reported to be superior to all other adsorbents.[18,19]

Graphene is known to have an sp^2 configuration and contain free π-bonds for the interaction with aromatic rings,[9] but the substance has not been yet studied for DBT adsorption. DBT was chosen because among the bulky sulfur compounds it is the most difficult to be removed.[18,19] This study, therefore, focuses mainly on the adsorption of DBT on graphene, with the latter being prepared using different synthesis procedures.

2. EXPERIMENTAL SECTION

2.1. Material Synthesis. For the synthesis of graphene, the following chemicals were used: graphite powder (Sigma-Aldrich, <45 μm, ≥99.99%), sulfuric acid (Sigma-Aldrich, ACS reagent, 95.0−98.0%), hydrochloric acid (Sigma-Aldrich,

Received: May 9, 2012
Revised: June 21, 2012
Accepted: July 6, 2012
Published: July 6, 2012

dx.doi.org/10.1021/ie301209c | *Ind. Eng. Chem. Res.* 2012, 51, 10259−10264

ACS reagent, 37%), hydrazine solution (Sigma-Aldrich, 35 wt % in H_2O), ammonia solution (Junsei, 28%, extra pure), sodium nitrate (Sigma-Aldrich, ≥99.0%), potassium permanganate (Samchun Chemical, 99.3%), ethanol (Sigma-Aldrich, ACS reagent, ≥99.5%, absolute), and phosphoric acid (Sigma-Aldrich, ACS reagent, ≥85 wt % in H_2O). For the desulfurization tests, toluene (Sigma-Alrich, CHROMASOLV, for HPLC, 99.9%) and dibenzothiophene (Sigma-Aldrich, ≥99%) were used; *n*-tetradecane (Kanto Chemical Co., Inc., ≥99.0%) was used as a solvent to dissolve DBT and toluene.

The widely used Hummers method for graphite oxide synthesis is as follows: Graphite powder (4.0 g) was mixed with 100 mL of H_2SO_4 in an ice bath. When the mixture temperature decreased to less than 10 °C, $KMnO_4$ (14.0 g) was added slowly. After stirring for 10 min, the oxidation process was conducted isothermally at 35 °C and maintained for 4 h. When the oxidation process was complete, the sample was transferred to an ice bath, and H_2O (150 mL) was added slowly (water reacting with sulfuric acid is highly exothermic). Then 50 mL of H_2O_2 was added and the mixture solution was stirred for 1 h. The resulting paste was centrifuged and washed five times with 37% HCl solution. Finally, it was washed with deionized water (150 mL) to achieve a pH ∼ 7. The product was frozen and then dried overnight in a vacuum oven at room temperature. In the following paragraphs, the graphite oxide produced by the Hummers method is indicated as "GOH".

Graphite oxide was also synthesized using a new method, which is a modified version of that by Marcano et al.[12] A sulfuric acid (Junsei, 360 mL) and phosphoric acid (Aldrich,40 mL) mixture was prepared in a round-bottom flask sitting on an ice bath, and 3.0 g of the graphite powder was added. When the temperature reached nearly 10 °C, 18.0 g of $KMnO_4$ was added slowly enough to prevent any sudden temperature increase. The mixture was stirred for 1 h and then transferred to a heating mantle to provide isothermal conditions at 45 °C. The oxidation process was conducted for 12 h; the system was then cooled to room temperature and placed in an ice bath. Finally, 400 mL of deionized water and 9 mL of 30% H_2O_2 were added gradually to the sample. The mixture turned bright yellow and generated copious bubbles. The mixture was stirred for 1 h and then centrifuged at 8000 rpm for 5 min. The remaining solid paste was washed with a mixture of 100 mL of deionized water, 100 mL of 30% HCl, and 100 mL of ethanol for 1 h, and this washing was repeated twice. The product was then washed twice with a mixture of 150 mL of deionized water and 150 mL of ethanol. The mixture was centrifuged at 8000 rpm after the washing procedure. After the washing steps, the paste was freeze- and vacuum-dried overnight. The graphite oxide obtained from this phosphoric acid based method is labeled "GOP".

Graphene samples made from GOH and GOP are labeled "GPH" and "GPP", respectively. One gram of each graphite oxide was dissolved in a solution of 500 mL of deionized H_2O and 1.5 mL of aqueous ammonia solution and then ultrasonicated for 1 h. Then 500 μL of hydrazine solution (35 wt % in H_2O, Sigma-Aldrich) was added, the mixture was cooled to room temperature, and then it was filtered through a 0.22 μm membrane filter (GVWP type, Millipore). The product was washed with 500 mL of deionized water for 1 h and then filtered again. The graphene powder was dried overnight in a vacuum chamber at room temperature.

2.2. Dibenzothiophene Adsorption Test. For the dibenzothiophene (DBT) adsorption reaction, 25 mg of graphene material was loaded into vials. Two milliliters of a model diesel solution (initial sulfur concentration of 377.1 ppm in *n*-tetradecane) and a modified commercial diesel (SK Energy, South Korea; initial sulfur level 8.99 ppmw) solution with initial sulfur concentration of 376.1 ppmw were loaded into the vials. The reactions were conducted in ultrasoniciation (Model Branson 5510) for 1 h. After the reaction was complete, the product mixture was filtered through a syringe filter (Puradisc 25 PP filter, Whatman; diameter 25 mm, pore size 0.2 μm) to collect the liquid product only. The product samples were analyzed in a trace sulfur analyzer [Model TS-100 V; Mitsubishi Chemical; analytical method, oxidative pyrolysis−ultraviolet fluorescence; furnace temperature 900−1000 °C; gas flow O_2 (391 mL/min), auxiliary gas (AUX) (177 mL/min), Ar (351 mL/min)].

2.3. Characterization. X-ray diffraction (XRD; Rigaku, 40 kV/100 mA of X-ray (step size 0.02°)) was used for adsorbent characterization; 5−60° of 2θ range was tested. Specific surface area (BET; ASAP 2400, Micromeritics) was estimated using nitrogen adsorption in the relative pressure range of 0.15−0.25 at 77 K. X-ray photoelectron spectroscopy (XPS; MultiLab 2000, Thermo) was carried out at 279−298 eV of the binding energy. Dispersive-Raman spectroscopy (Model LabRAM HR UV/vis/NIR) was carried out with an Ar ion continuous wave laser (514.5 nm).

3. RESULTS AND DISCUSSION

3.1. Characterization of Graphene Depending on Preparation Methods. Figures 1 and 2 show the XRD patterns for graphite oxide and graphene, respectively. The interlayer *d*-spacing between the graphitic layers should be an indicator of the degree of oxidation of graphite oxide. Oxygen-containing functional groups, such as hydroxyl, epoxy, and carboxyl groups, on and between graphite layers enlarge the interlayer spacing of the graphite layers[20] and turn the graphite oxide to an sp^3 configuration. A larger interlayer spacing should therefore indicate a higher degree of oxidation of the graphite oxide. The interlayer spacing (*d*-spacing) has been calculated from Bragg's law. A typical interlayer spacing for GO has been reported as 7−8 Å.[20−22] An earlier study[12] confirmed that the *d*-spacing for the graphite oxide produced with H_3PO_4 has a larger *d*-spacing than for that synthesized using the Hummers method. In this study, the (002) peak[23] for GOH and that for

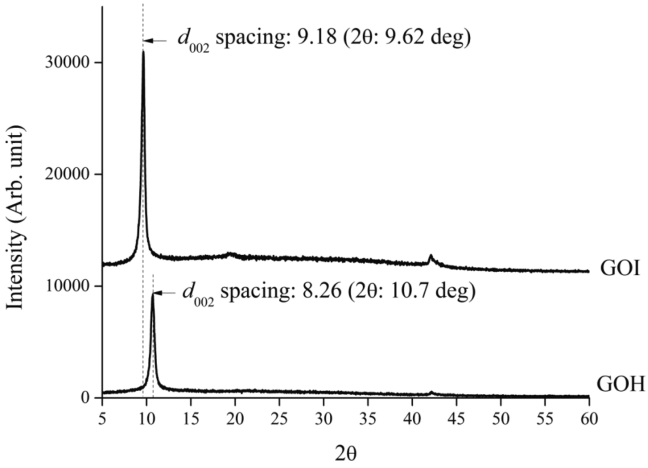

Figure 1. XRD for graphite oxide and interlayer *d*-spacing.

dx.doi.org/10.1021/ie301209c | *Ind. Eng. Chem. Res.* 2012, 51, 10259−10264

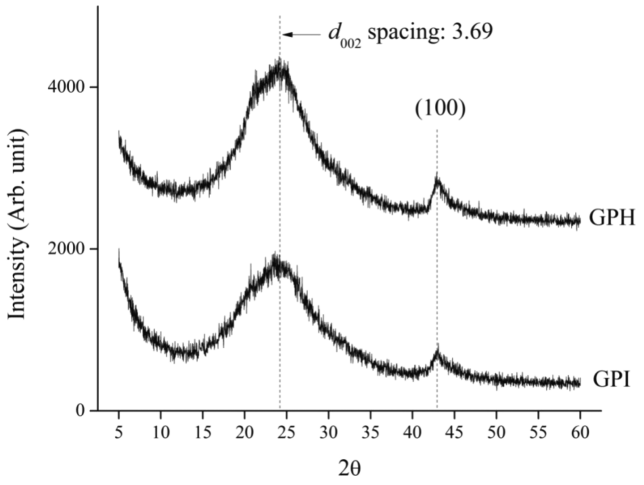

Figure 2. XRD of graphene and interlayer *d*-spacing.

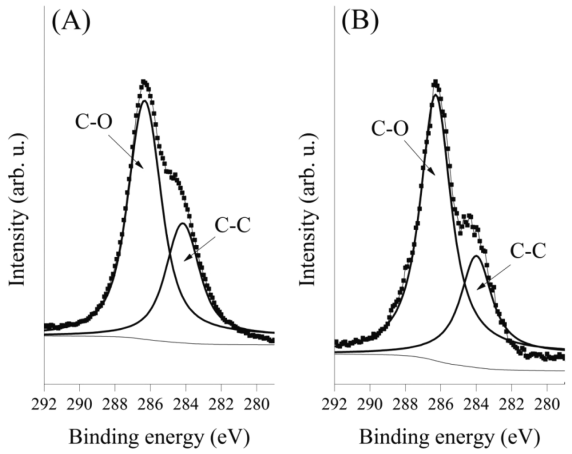

Figure 3. XPS of graphite oxide: (A) GOH and (B) GOP.

GOP were located at 10.7° and 9.6°, corresponding to interlayer *d*-spacings of 8.2 and 9.2 Å, respectively. Since the typical spacing between the graphite layers is known to be 3.4 Å,[24] the larger *d*-spacing for the graphite oxides implies that the oxygen-containing functional groups occur between the graphite oxide layers. It can also be seen that the graphite oxides with H_3PO_4 (GOP) have a larger interlayer spacing than that of the graphite oxide obtained from the Hummers method (GOH). Once the graphite oxide layers are exfoliated and reduced, they return to an sp^2 layer structure. Therefore, the intensity of the graphite oxide peak completely disappeared in the XRD pattern of graphene, characterized by a broad peak centered around 24° and corresponding to an interlayer *d*-spacing of 3.69 Å with (002) structure.[25,26] This result could indicate the recovery of graphitic crystal structure.[21] Table 1 shows the overall crystallite size (L_a) and thickness (L_c) of graphite oxide and graphene calculated from the Scherrer equation: For the graphite oxides, the overall size (L_a) is larger and thicker (L_c) than for graphene. It can be concluded that the oxygen-containing functional groups on the surface of the graphite oxide are removed; then the graphene layers are exfoliated from each other, leading to a smaller number of graphene layers. It is also supported from BET analysis since GPP which has a fewer number of layers possesses a higher specific surface area of 853.9 m^2/g than GPH (394.9 m^2/g).

The binding energies of the C 1s levels of the graphite oxides were determined by XPS and are shown in Figure 3. The degree of oxidation of graphite oxide can be determined from the ratio of the areas under the curve for C−C and C−O (including epoxy and hydroxyl groups) located at 284.4 and 286.2 eV, respectively.[27] Depending on the synthesis methods, the ratio of oxygen to carbon varies, as shown in Table 2. The quantitative fractions, C−O bonds to C−C bonds ratio, of the GOH and GOP are 2.08 and 2.69, respectively. This confirms that GOP has a higher degree of oxidation than the graphite oxide obtained from the Hummers method (GOH). To obtain graphene, the oxygen-containing functional groups attached to two neighboring graphene layers are reduced in a hydrazine aqueous solution environment, a process that transforms the sp^3 bonds to sp^2 bonds. The graphene layers are then detached from each other. As a result, two types of graphenes, GPH, obtained from GOH, and GPP, reduced from GOP, were obtained. The XPS analysis, Figure 4, confirmed that the degree of oxidation of GPH and GPP decreased from ~2 to 0.15. It is difficult to distinguish the quantitative difference between GPH and GPP from XPS analysis since most of the oxygen-containing functional groups between the layers were removed by the reduction process.

Table 2. XPS Fitting Analysis for Graphite Oxide and Graphene

	binding energy (eV)	GOH (area)	GOP (area)	GPH (area)	GPP (area)
C−C	284.18	57 507	3 328	361 316	205 309
C−O	286.33	119 609	8 939	54 129	30 325
ratio of C−O/C-C		2.08	2.69	0.15	0.15

Raman spectroscopic analysis has been chosen to probe the structural and electronic characteristics of graphitic materials[28] because it provides information on in-plane bond stretching of sp^2 carbon atoms in both rings and chains (G band in the range 1500−1600 cm^{-1}), information on the defects from the breathing modes of sp^2 atoms in hexagonal rings (D band in the range 1200−1500 cm^{-1}), and information on the stacking order (2D band).[29] The Raman G band can be attributed therefore to graphitic sp^2 bonded carbon, and the D band is also widely used for determining the thickness of graphene

Table 1. Surface Area and Overall Crystallite Size (L_a and L_c) Analysis

		XRD							
		(002) plane					(100) plane		
	BET surf. area (m^2/g)	2θ (deg)	width (deg)	L_c (nm)	*d*-spacing (Å)	no. of layers	2θ (deg)	width (deg)	L_a (nm)
GOH	–	10.7	0.5	35	8.3	42.4	42.2	0.2	163.5
GOP	–	9.6	0.4	39	9.2	42.5	42.1	0.3	141.7
GPH	394.9	24.1	7.4	2.3	3.7	6.2	42.9	0.9	40.0
GPP	853.9	23.6	11.6	1.5	3.8	3.9	43.1	0.7	50.1

dx.doi.org/10.1021/ie301209c | *Ind. Eng. Chem. Res.* 2012, 51, 10259−10264

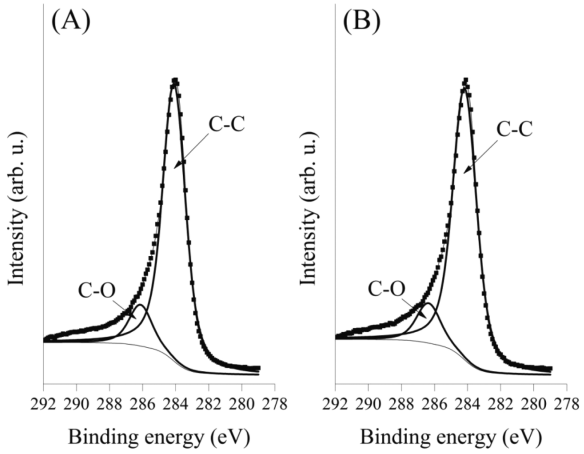

Figure 4. XPS of graphene: (A) GPH and (B) GPP.

materials.[30] Figure 5 shows Raman spectroscopic results obtained with an excitation wavelength of 514.5 nm for

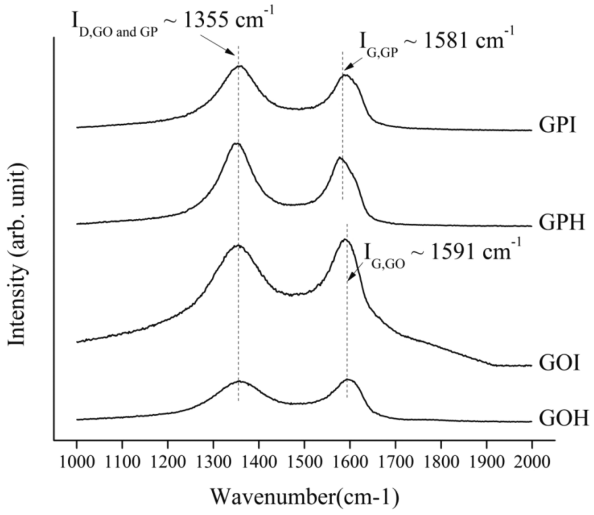

Figure 5. Raman spectroscopy of graphite oxide and graphene.

graphite oxide and graphene. All samples were deposited on silicon wafers in powder form without the use of a solvent. Graphite has a single G band at 1580 cm^{-1}.[20] When graphite was oxidized to graphite oxide, the G band peak shifted from 1580 to 1591 cm^{-1}, and the D band intensity at 1355 cm^{-1} increased due to the resonance of isolated double bonds on graphite oxide.[31] After the graphite oxide was reduced to a 2D graphene layer, the G band returned from 1591 to 1581 cm^{-1}.The structural changes from graphite oxide to graphene (i.e., the graphitization degree of carbonaceous materials and the defect density[32]) could be observed by comparing the intensity ratio of the D and G bands (I_D/I_G). I_D/I_G ratios for GOH and GOP were 0.94 and 0.95, respectively. In addition, I_D/I_G ratios for GPH and GPP were 1.25 and 1.12, respectively. In agreement with previous reports for graphite oxides and graphene, the ratio of I_D/I_G increases when the graphite oxide is reduced to graphene.[33,34] This result indicates that the chemical reduction of graphite oxide increases the number of small regions of aromatic compounds that can be detected from the D band. Also, the ratio I_D/I_G for GPP is lower than that for GPH, implying, perhaps, that GPP has fewer defects than GPH and/or larger overall size. This hypothesis is supported by the L_a and L_c results (Table 1) calculated from the Scherrer equation.[34]

3.2. Selective Adsorption of Sulfur Compounds on Graphene. Given the characterizations described, GOP, which has the larger interlayer *d*-spacing, should be more easily reduced than GOH. GPP has fewer defects (larger L_a) and is thinner (smaller L_c), resulting in a higher specific surface area than GPH. It can be concluded therefore that GPP should have a better structural integrity for sp^2 configuration (possessing π-bonds) than GPH. In other words, for an identical mass of graphene, GPP should have a greater density of π-bonds than GPH. Since $\pi-\pi$ interaction is important for adsorbing bulky thiophenes,[18,19] it was decided to characterize further both GPP and GPH through their capacity to adsorb dibenzothiophene (Figure 6).

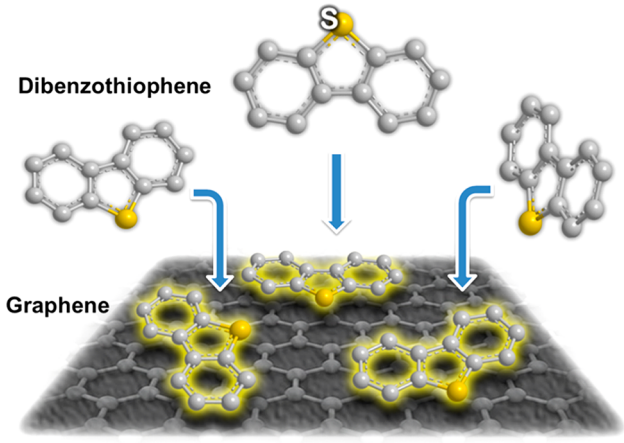

Figure 6. Schematic illustration of the adsorption of DBT on graphene.

Dibenzothiophene (DBT), which has two aromatic rings with thiophene, can be adsorbed via $\pi-\pi$ interaction.[35,36] Our results suggest that GPP has more available π-bonds than GPH does. Figure 7 shows DBT adsorption results obtained using commercial diesel and model diesel solutions. The initial sulfur concentration for the model solution was set at 377.1 ppmw. Because graphite oxide has an sp^3 configuration (no available π-bonds for the adsorption), the raw graphite and graphite oxides cannot adsorb DBT, even though DBT has π-bonds from both

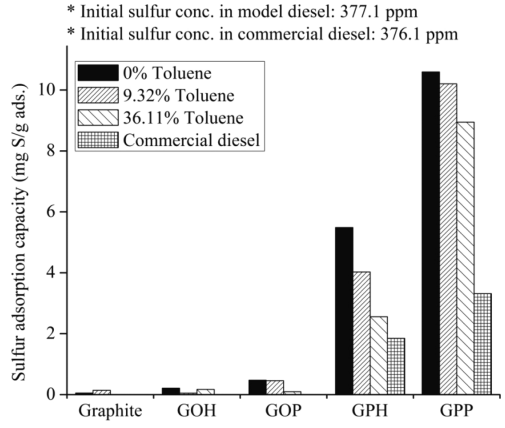

Figure 7. DBT adsorption on graphene using a model and commercial diesel solution.

dx.doi.org/10.1021/ie301209c | *Ind. Eng. Chem. Res.* 2012, 51, 10259−10264

aromatic rings. However, the DBT compounds were adsorbed on the surface of graphene, a fact that confirms that π-bonds (sp^2 carbon configuration) are needed for the adsorption of DBT compounds. It was found that, depending on the synthesis methods of the graphite oxide, the adsorption capacity of DBT on graphene is affected. Our results indicate that the adsorption capacity of GPP (10.6 mg of S/g of adsorbent) has almost twice that of GPH (5.5 mg of S/g of adsorbent), with an initial sulfur concentration of 377.1 ppm. Since a commercial diesel fuel contains only 8.99 ppm sulfur, extra DBT was added for the adsorption tests, resulting in a total initial sulfur concentration of 376.1 ppm. Since commercial diesel contains many aromatic compounds, it is anticipated that the DBT adsorption capacity obtained with commercial diesel will be lower than that obtained with a model diesel. Using commercial diesel, GPH and GPP showed adsorption capacities of 1.85 and 3.31 mg of S/g of adsorbent, respectively. Even in a very severe environment (a commercial diesel fuel), therefore, graphene shows a sulfur adsorption capacity even though the amount of sulfur adsorbed is much less than when using the model diesel. To investigate the selectivity of DBT, the effect of toluene (aromatic compound) was tested by adding different concentrations of toluene: 9 and 36 wt % toluene in *n*-tetradecane solvent. The results (Figure 7) show as expected that toluene interfered with the adsorption of DBT: as the toluene concentration increased, the DBT adsorption decreased.

4. CONCLUSION

The characteristics of graphite oxide and graphene can be changed depending on the preparation method used. The interlayer *d*-spacing for graphite oxide especially can be controlled by the synthesis method. The overall crystallite size and thickness of graphite oxide and graphene were calculated. Synthesizing graphite oxide with H_3PO_4 (GOP) led to a higher degree of oxidation than synthesizing it by the Hummers method (GOH), as confirmed by XPS analysis. GOP led to a larger crystallite size and thinner graphene than GOH. It has been confirmed that graphite oxide which has a larger interlayer spacing (GOP) is able to produce a higher quality graphene possessing a higher surface area, larger overall size, and thinner thickness. DBT adsorption tests were carried out for a model diesel compound and a commercial diesel. The graphite oxide, which has an sp^3 configuration, did not adsorb DBT compounds. However, graphene materials, which have an sp^2 configuration, were able to adsorb DBT compounds via $\pi-\pi$ interactions. Graphene which has a higher surface area and thinner thickness (GPP) showed a higher DBT adsorption capacity than GPH. The graphene adsorption capacity was lower for the commercial diesel than for the model diesel compound, a fact attributed to the presence of many other aromatic compounds in commercial diesel. The reduced DBT adsorption selectivity in the presence of aromatic compounds was confirmed by performing DBT adsorption tests in the presence of different toluene concentrations.

AUTHOR INFORMATION

Corresponding Author

*Tel.: +1 (519) 888-4567 (ext 36472) (E.C.); +82 62-530-1873 (C.H.K.). Fax: +1 (519) 888-4567 (E.C.); +82 62-530-1889 (C.H.K.). E-mail: ecroiset@uwaterloo.ca (E.C.); chko@jnu.ac.kr (C.H.K.).

Notes

The authors declare no competing financial interest.

ACKNOWLEDGMENTS

This research was supported by Basic Science Research Program through the National Research Foundation of Korea (NRF) funded by the Ministry of Education, Science and Technology (2012R1A1A4A01019828).

REFERENCES

(1) Zhu, X.; Zhu, Y.; Murali, S.; Stoller, M. D.; Ruoff, R. S. Nanostructured Reduced Graphene Oxide/Fe_2O_3 Composite as a High-Performance Anode Material for Lithium Ion Batteries. *ACS Nano* **2011**, *5*, 3333.

(2) Dubin, S.; Gilje, S.; Wang, K.; Tung, V. C.; Cha, K.; Hall, A. S.; Farrar, J.; Varshneya, R.; Yang, Y.; Kaner, R. B. A One-Step, Solvothermal Reduction Method for Producing Reduced Graphene Oxide Dispersions in Organic Solvents. *ACS Nano* **2010**, *4*, 3845.

(3) Khan, U.; O'Connor, I.; Gun'ko, Y. K.; Coleman, J. N. The Preparation of Hybrid Films of Carbon Nanotubes and Nano-Graphite/Graphene with Excellent Mechanical and Electrical Properties. *Carbon* **2010**, *48*, 2825.

(4) Stankovich, S.; Piner, R.; Nguyen, S. T.; Ruoff, R. S. Synthesis and Exfoliation of Isocyanate-treated Graphene Oxide Nanoplatelets. *Carbon* **2006**, *44*, 3342.

(5) Talyzin, A. V.; Sundqvist, B.; Szabo, T.; Dmitriev, V. Structural Breathing of Graphite Oxide Pressurized in Basic and Acidic Solutions. *J. Phys. Chem. Lett.* **2011**, *2*, 309.

(6) Lee, J. K.; Smith, K. B.; Hayner, C. M.; Kung, H. H. Silicon Nanoparticles-Graphene Paper Composites for Li Ion Battery Anodes. *Chem. Commun.* **2010**, *46*, 2025.

(7) Wang, D.; Choi, D.; Li, J.; Yang, Z.; Nie, Z.; Kou, R.; Hu, D.; Wang, C.; Saraf, L. V.; Zhang, J.; Aksay, I. A.; Liu, J. Self-Assembled TiO_2−Graphene Hybrid Nanostructures for Enhanced Li-Ion Insertion. *ACS Nano* **2009**, *3*, 907.

(8) Hummers, W. S. J.; Offeman, R. E. Preparation of Graphitic Oxide. *J. Am. Chem. Soc.* **1958**, *80*, 1339.

(9) Xu, Y.; Bai, H.; Lu, G.; Li, C.; Shi, G. Flexible Graphene Films via the Filtration of Water-Soluble Noncovalent Functionalized Graphene Sheets. *J. Am. Chem. Soc.* **2008**, *130*, 5856.

(10) Yan, J.; Fan, Z.; Wei, T.; Qian, W.; Zhang, M.; Wei, F. Fast and Reversible Surface Redox Reaction of Graphene−MnO_2 Composites as Supercapacitor Electrodes. *Carbon* **2010**, *48*, 3825.

(11) Kuilla, T.; Bhadra, S.; Yao, D.; Kim, N. H.; Bose, S.; Lee, J. H. Recent Advances in Graphene Based Polymer Composites. *Prog. Polym. Sci.* **2010**, *35*, 1350.

(12) Marcano, D. C.; Kosynkin, D. V.; Berlin, J. M.; Sinitskii, A.; Sun, Z.; Slesarev, A.; Alemany, L. B.; Lu, W.; Tour, J. M. Improved Synthesis of Graphene Oxide. *ACS Nano* **2010**, *4*, 4806.

(13) Takahashi, A.; Yang, F. H.; Yang, R. T. New Sorbents for Desulfurization by π-Complexation: Thiophene/Benzene Adsorption. *Ind. Eng. Chem. Res.* **2002**, *41*, 2487.

(14) Yang, R. T.; Hernández-Maldonado, A. J.; Yang, F. H. Desulfurization of Transportation Fuels with Zeolites under Ambient Conditions. *Science* **2003**, *301*, 79.

(15) Yu, G.; Lu, S.; Chen, H.; Zhu, Z. Diesel Fuel Desulfurization with Hydrogen Peroxide Promoted by Formic Acid and Catalyzed by Activated Carbon. *Carbon* **2005**, *43*, 2285.

(16) Chen, H.; Zhou, X.; Shang, H.; Liu, C.; Qiu, J.; Wei, F. Study of Dibenzothiophene Adsorption over Carbon Nanotube Supported CoMo HDS Catalysts. *J. Nat. Gas Chem.* **2004**, *13*, 209.

(17) Laborde-Boutet, C.; Joly, G.; Nicolaos, A.; Thomas, M.; Magnoux, P. Selectivity of Thiophene/Toluene Competitive Adsorptions onto NaY and NaX Zeolites. *Ind. Eng. Chem. Res.* **2006**, *45*, 6758.

(18) Hernández-Maldonado, A. J.; Yang, R. T. Desulfurization of Commercial Liquid Fuels by Selective Adsorption via π-Complexation with Cu(I)-Y Zeolite. *Ind. Eng. Chem. Res.* **2003**, *42*, 3103.

(19) Wang, Y.; Yang, R.; Heinzel, J. Desulfurization of Jet Fuel by π-complexation Adsorption with Metal Halides Supported on MCM-41 and SBA-15 Mesoporous Materials. *Chem. Eng. Sci.* **2008**, *63*, 356.
(20) Kudin, K. N.; Ozbas, B.; Schniepp, H. C.; Prud'homme, R. K.; Aksay, I. A.; Car, R. Raman Spectra of Graphite Oxide and Functionalized Graphene Sheets. *Nano Lett.* **2008**, *8*, 36.
(21) Long, D.; Li, W.; Ling, L.; Miyawaki, J.; Mochida, I.; Yoon, S.-H. Preparation of Nitrogen-Doped Graphene Sheets by a Combined Chemical and Hydrothermal Reduction of Graphene Oxide. *Langmuir* **2010**, *26*, 16096.
(22) Wakeland, S.; Martinez, R.; Grey, J. K.; Luhrs, C. C. Production of Graphene from Graphite Oxide using Urea as Expansion−Reduction Agent. *Carbon* **2010**, *48*, 3463.
(23) Wu, J.; Bai, S.; Shen, X.; Jiang, L. Preparation and Characterization of Graphene/CdS Nanocomposites. *Appl. Surf. Sci.* **2010**, *257*, 747.
(24) Srinivas, G.; Zhu, Y.; Piner, R.; Skipper, N.; Ellerby, M.; Ruoff, R. Synthesis of Graphene-like Nanosheets and Their Hydrogen Adsorption Capacity. *Carbon* **2010**, *48*, 630.
(25) Wang, J.-Z.; Zhong, C.; Chou, S.-L.; Liu, H.-K. Flexible Free-Standing Graphene-Silicon Composite Film for Lithium-Ion Batteries. *Electrochem. Commun.* **2010**, *12*, 1467.
(26) Hontoria-Lucas, C. Study of Oxygen-Containing Groups in a Series of Graphite Oxides: Physical and Chemical Characterization. *Carbon* **1995**, *33*, 1585.
(27) Liao, K.-H.; Mittal, A.; Bose, S.; Leighton, C.; Mkhoyan, K. A.; Macosko, C. W. Aqueous Only Route Toward Graphene from Graphite Oxide. *ACS Nano* **2011**, *5*, 1253.
(28) Ni, Z.; Wang, Y.; Yu, T.; Shen, Z. Raman Spectroscopy and Imaging of Graphene. *Nano Res.* **2010**, *1*, 273.
(29) Ferrari, A. Raman Spectroscopy of Graphene and Graphite: Disorder, Electron−Phonon Coupling, Doping and Nonadiabatic Effects. *Solid State Commun.* **2007**, *143*, 47.
(30) Zickler, G. A.; Smarsly, B.; Gierlinger, N.; Peterlik, H.; Paris, O. A Reconsideration of the Relationship between the Crystallite Size La of Carbons Determined by X-ray Diffraction and Raman Spectroscopy. *Carbon* **2006**, *44*, 3239.
(31) Choi, S. M.; Seo, M. H.; Kim, H. J.; Kim, W. B. Synthesis of Surface Functionalized Graphene Nanosheets with High Pt-loadings and Their Applications to Methanol Electrooxidation. *Carbon* **2010**, *49*, 904.
(32) Zhang, M.; Lei, D.; Du, Z.; Yin, X.; Chen, L.; Li, Q.; Wang, Y.; Wang, T. Fast Synthesis of SnO_2/Graphene Composites by Reducing Graphene Oxide with Stannous Ions. *J. Mater. Chem.* **2011**, *21*, 1673.
(33) Higginbotham, A. L.; Kosynkin, D. V.; Sinitskii, A.; Sun, Z.; Tour, J. M. Lower-Defect Graphene Oxide Nanoribbons from Multiwalled Carbon Nanotubes. *ACS Nano* **2010**, *4*, 2059.
(34) Saner, B.; Dinç, F.; Yürüm, Y. Utilization of Multiple Graphene Nanosheets in Fuel Cells: 2. The Effect of Oxidation Process on the Characteristics of Graphene Nanosheets. *Fuel* **2011**, *90*, 2609.
(35) Bjork, J.; Hanke, F.; Palma, C.-A.; Samori, P.; Cecchini, M.; Persson, M. Adsorption of Aromatic and Anti-Aromatic Systems on Graphene through π−π Stacking. *J. Phys. Chem. Lett.* **2010**, *1*, 3407.
(36) Jeong, H.-K.; Lee, Y. P.; Lahaye, R. J. W. E.; Park, M.-H.; An, K. H.; Kim, I. J.; Yang, C.-W.; Park, C. Y.; Ruoff, R. S.; Lee, Y. H. Evidence of Graphitic AB Stacking Order of Graphite Oxides. *J. Am. Chem. Soc.* **2008**, *130*, 1362.